

Experimental Progress in Hypernuclear Physics

Hirokazu TAMURA

Department of Physics, Tohoku University, Sendai 980-8578, Japan

Recent experimental progress of hypernuclear physics is reviewed. Detailed level structure of various p -shell Λ hypernuclei has been investigated by γ -ray spectroscopy with Hyperball and an NaI counter array, and the strengths of all the spin-dependent components of the ΛN interaction have been determined. The $(e, e' K^+)$ reaction has been successfully introduced to hypernuclear spectroscopy at Jefferson Laboratory with a resolution better than 1 MeV (FWHM). The first experiment with the (π^-, K^+) reaction was carried out at KEK to produce neutron-rich hypernuclei. Double hypernuclear events interpreted as ${}^4_{\Lambda\Lambda}\text{H}$ were observed by detecting two π^- 's from sequential weak decay. In an emulsion-counter hybrid experiment, a double Λ hypernucleus ${}^6_{\Lambda\Lambda}\text{He}$ was observed and the strength of the $\Lambda\Lambda$ interaction was unambiguously derived. A series of KEK experiments studying weak decays of ${}^5_{\Lambda}\text{He}$ and ${}^{12}_{\Lambda}\text{C}$ have solved the so-called Γ_n/Γ_p ratio puzzle.

§1. Introduction

1.1. Interest of hypernuclear physics

The objective of hypernuclear physics is to extend our understanding of atomic nucleus as a many-body system of protons and neutrons into a many-body system of baryons including hyperons so as to give more generalized descriptions of matter.

The starting point to study many-body systems including hyperons (Y) is to investigate YN and YY interactions, of which experimental information is quite limited because of difficulties in YN scattering experiments. The experimental data on hypernuclear structure provide rich information on the interactions; the interactions constructed from NN scattering data with a guidance of the flavor $SU(3)$ symmetry are tested and improved with hypernuclear data. The ultimate goal of the study of YN and YY interactions is to understand the baryon-baryon interactions in a unified way. Such studies will also enable us to understand the origin of the short-range nuclear force, which may be described by quark-gluon picture rather than meson-exchange picture.

The next step is to explore many-body systems with one or more strangeness. Properties of nuclei and nuclear matter may be drastically changed when many hyperons are included in the system. It is speculated that hyperons stably exist in high density nuclear matter inside a neutron star because a neutron Fermi energy can possibly exceed the hyperon-nucleon mass difference. Nuclear matter with strangeness is thus a doorway to explore high density nuclear matter. On the other hand, even a single hyperon added to a nucleus can modify nuclear properties, such as size, shape, symmetry, cluster and halo/skin structure, etc. Such "impurity effects" are induced by the properties of hyperons that they are free from the Pauli effect in a nucleus and feel nuclear forces different from the NN force.

Another important aspect of hypernuclear physics is to use hypernuclei as a laboratory to study properties and interactions of baryons. The nonmesonic weak

decay of hypernuclei via $\Lambda N \rightarrow NN$ provides a unique opportunity to study baryon-baryon weak interaction. It can be understood in the framework of the YN interaction models, but short-range forces are expected to play more important roles here. In addition, since a hyperon can stay deeply in a nucleus but distinguishable from nucleons, it can be a probe to investigate possible modifications of baryons in nuclear matter. For example, a magnetic moment of a Λ inside a nucleus will provide us with a clue to understand partial restoration of chiral symmetry and the origin of the magnetic moment of baryons.

1.2. Recent experiments

In these several years, great progress has been made in hypernuclear physics from both experimental and theoretical sides. The experimental progress results from recently-developed new methods and techniques. Table I lists experiments on strangeness nuclear physics carried out in these five years. In the followings, this article focuses on the experiments related to Λ and $\Lambda\Lambda$ hypernuclei. In particular, γ spectroscopy of Λ hypernuclei is discussed more in detail.

Table I. List of experiments for strangeness nuclear physics since 1998. Only experiments that have finished data-taking are shown.

Experiment	Year of run	Line/Apparatus	Target/Reaction	Objects	Ref.
γ spectroscopy of Λ hypernuclei					
KEK E419	1998	K6,SKS,Hyperball	${}^7\text{Li}(\pi^+, K^+\gamma)$	${}^7_{\Lambda}\text{Li}$	1)–3)
BNL E929	1998	D6,NaI array	${}^{13}\text{C}(K^-, \pi^-\gamma)$	${}^{13}_{\Lambda}\text{C}$	4)
BNL E930('98)	1998	D6,Hyperball	${}^9\text{Be}(K^-, \pi^-\gamma)$	${}^9_{\Lambda}\text{Be}$	5)
BNL E930('01)	2001	D6,Hyperball	${}^{16}\text{O}, {}^{10}\text{B}(K^-, \pi^-\gamma)$	${}^{16}_{\Lambda}\text{O}, {}^{15}_{\Lambda}\text{N}, {}^{10}_{\Lambda}\text{B}, \dots$	6), 7)
KEK E509	2002	K5,Hyperball	${}^9\text{Be}, {}^{10}\text{B}, \dots (K^-_{stop}, \gamma)$	${}^7_{\Lambda}\text{Li}, \dots$	8)
KEK E518	2002	K6,SKS,Hyperball	${}^{11}\text{B}(\pi^+, K^+\gamma)$	${}^{11}_{\Lambda}\text{B}$	9)
$(e, e'K^+)$ spectroscopy of Λ hypernuclei					
Jlab E89-009	1999	Hall-C,HNSS	${}^{12}\text{C}(e, e'K^+)$	${}^{12}_{\Lambda}\text{B}$	10)
neutron-rich Λ hypernuclei					
KEK E521	2002-3	K6, SKS	${}^{10}\text{B}(\pi^-, K^+)$	${}^{10}_{\Lambda}\text{Li}$	11)
$\Lambda\Lambda$ hypernuclei					
BNL E906	1998	D6,CDS	${}^9\text{Be}(K^-, K^+\pi^-\pi^-)$	${}^4_{\Lambda\Lambda}\text{H}$	12)
KEK E373	1998-00	K2,emulsion	$\text{C}+\text{emulsion}(K^-, K^+)$	${}^6_{\Lambda\Lambda}\text{He}, \dots$	13)
weak decay of Λ hypernuclei					
BNL E931	2001-2	C6,NMS	${}^4\text{He}(K^-_{stop}, \pi^0 N)$	${}^4_{\Lambda}\text{H}$	14)
KEK E462	2000-1	K6,SKS	${}^6\text{Li}(\pi^+, K^+\pi^-/N)$	${}^5_{\Lambda}\text{He}$	15)–17)
KEK E508	2002	K6,SKS	${}^{12}\text{C}(\pi^+, K^+\pi^-/N)$	${}^{12}_{\Lambda}\text{C}$	15), 16)
Σ hypernuclei					
KEK E438	1999	K6,SKS	${}^{28}\text{Si}, \dots {}^{208}\text{Pb}(\pi^-, K^+)$	Σ -Nucleus	18)
YN scattering					
KEK E452	2000-1	K2	${}^{12}\text{C}(\pi, K^+)\Lambda, \Sigma$	$\Lambda, \Sigma + p$ (${}^{12}\text{C}$)	19), 20)
\bar{K} -nucleus bound states					
BNL E930 _{para}	2001	D6	${}^{16}\text{O}(K^-, n)$	${}^{15}_{\bar{K}}\text{N}$	21)
KEK E471	2002-3	K5	${}^4\text{He}(K^-_{stop}, n)$	${}^3_{\bar{K}}\text{H}$	22)

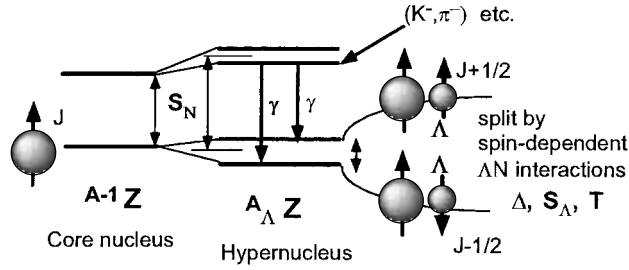


Fig. 2. Hypernuclear fine structure and γ spectroscopy. High resolution of Ge detector is essential to resolve two levels (“hypernuclear fine structure”) split by ΛN spin-dependent interactions. See text for details.

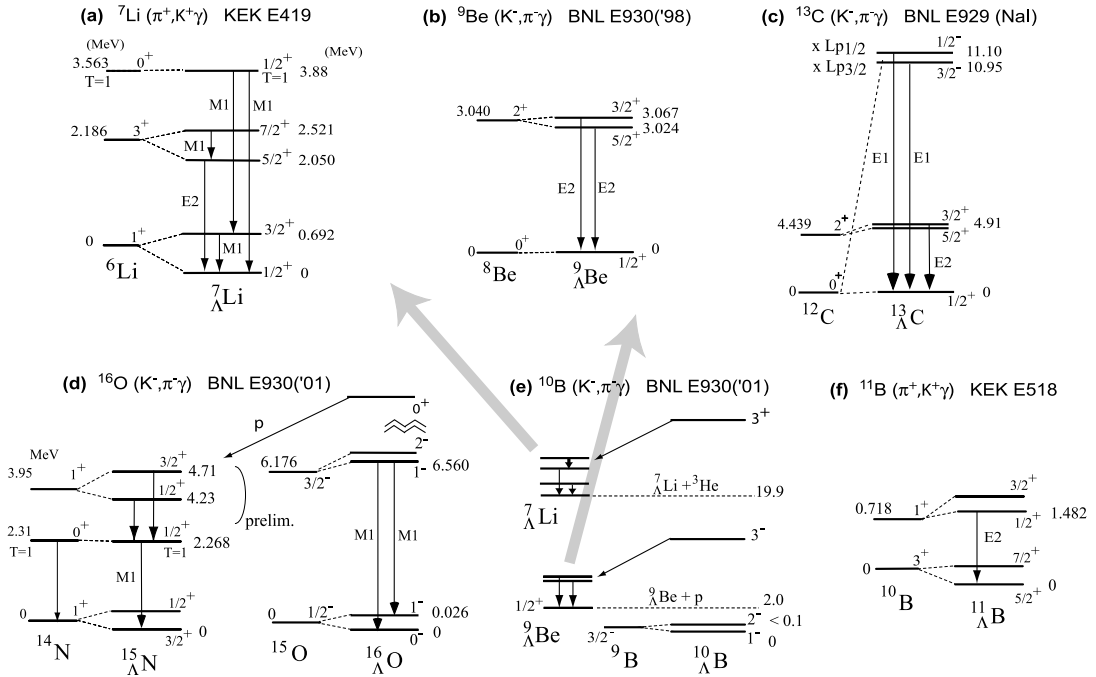


Fig. 3. Level schemes of ${}^7_\Lambda\text{Li}$, ${}^9_\Lambda\text{Be}$, ${}^{10}_\Lambda\text{B}$, ${}^{11}_\Lambda\text{B}$, ${}^{13}_\Lambda\text{C}$, ${}^{15}_\Lambda\text{N}$ and ${}^{16}_\Lambda\text{O}$ determined from recent γ -ray experiments.

orbit term, the nucleon-spin-dependent spin-orbit term and the tensor term.^{23),24)} By comparing experimental level energies with shell-model calculations, these integrals (parameters) can be experimentally determined; the values of Δ , S_Λ and T are derived from the spacing of the doublet, while the S_N value is given by change of the level spacing in the core nucleus.

Figure 3 shows all the hypernuclear γ transitions observed in recent experiments. γ rays in ${}^{13}_\Lambda\text{C}$ were observed with an NaI array, and all the other γ rays were observed with Hyperball. We plan to extend this figure to a book of “Table of Hyper-Isotopes” through further study of hypernuclear γ spectroscopy.

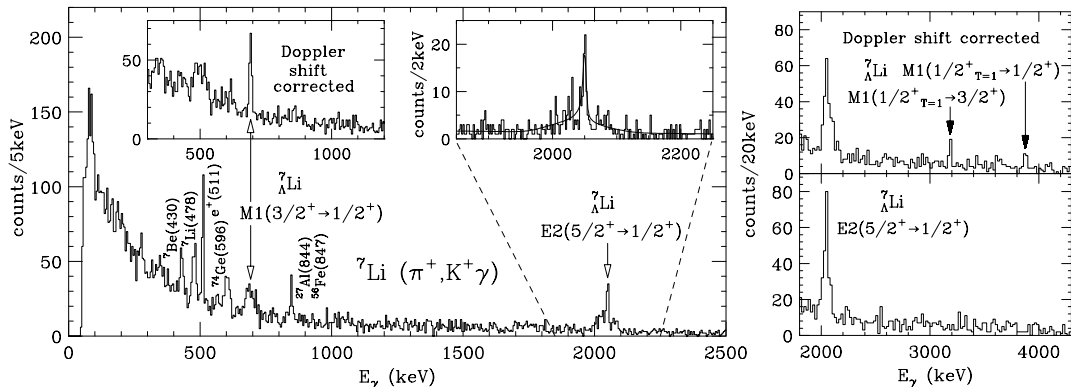


Fig. 4. γ -ray spectrum of ${}^7_{\Lambda}\text{Li}$ measured with Hyperball in KEK E419. The $M1(\frac{3}{2}^+ \rightarrow \frac{1}{2}^+)$, $E2(\frac{5}{2}^+ \rightarrow \frac{1}{2}^+)$, $M1(\frac{1}{2}^+(T=1) \rightarrow \frac{3}{2}^+)$, and $M1(\frac{1}{2}^+(T=1) \rightarrow \frac{1}{2}^+)$ transitions were observed. The γ -ray peak at 429 keV is attributed to the transition in ${}^7\text{Be}$ after the weak decay of ${}^7_{\Lambda}\text{Li} \rightarrow {}^7\text{Be}(429) + \pi^-$. Right inset in the left figure shows the fitting of the $E2$ peak with a partly Doppler-broadened peak shape (simulation) for the optimum lifetime of 5.8 ps.

2.2. ${}^7_{\Lambda}\text{Li}$ — The best studied hypernucleus

${}^7_{\Lambda}\text{Li}$ is the hypernucleus which has been best studied by γ spectroscopy. Five γ transitions of ${}^7_{\Lambda}\text{Li}$ were observed, and the complete level scheme for all the bound states with energies and spins was determined as shown in Fig. 3 (a). In addition, the $B(E2)$ value was also measured.

In the first experiment with Hyperball (KEK E419), four γ -ray peaks were observed at 692 keV, 2050 keV, 3186 keV, and 3877 keV.¹⁾ They are uniquely assigned as the Λ -spin-flip $M1(3/2^+ \rightarrow 1/2^+)$ transition, the $E2(5/2^+ \rightarrow 1/2^+)$ transition, the $M1(1/2^+(T=1) \rightarrow 3/2^+)$ transition, and the $M1(1/2^+(T=1) \rightarrow 1/2^+)$ transition, respectively.

The energy spacing of the ground-state doublet ($3/2^+, 1/2^+$) gives the strength of the ΛN spin-spin interaction, $\Delta = 0.43$ MeV, by comparing the experimental value of 692 keV with a shell-model calculation by Millener (an updated version with the $\Sigma\Lambda$ coupling effect).²⁵⁾ This result gives a strong constraint to baryon-baryon interaction models as described in §2.6.

On the other hand, from the peak shape of the $E2(\frac{5}{2}^+ \rightarrow \frac{1}{2}^+)$ γ ray at 2050 keV, the lifetime of the $\frac{5}{2}^+$ state was derived to be $5.8^{+0.9}_{-0.7}(\text{stat}) \pm 0.7(\text{syst})$ ps with the Doppler shift attenuation method. It is then converted to a $B(E2)$ value of $3.6 \pm 0.5^{+0.5}_{-0.4} e^2\text{fm}^4$.²⁾ This is the first measurement of reduced transition probabilities of hypernuclei. This $B(E2)$ value is three times smaller than the $B(E2)$ for the corresponding core nucleus transition ${}^6\text{Li}(3^+ \rightarrow 1^+)$ ($10.9 \pm 0.9 e^2\text{fm}^4$), which indicates a significant shrinkage of the ${}^7_{\Lambda}\text{Li}$ size from the ${}^6\text{Li}$ size. More description is found in Ref. 2). According to a recent cluster-model calculation,²⁶⁾ the measured $B(E2)$ corresponds to a shrinkage of the distance between the α cluster and the center of mass for p and n by $19 \pm 4\%$. Thus the phenomenon of nuclear shrinkage induced by

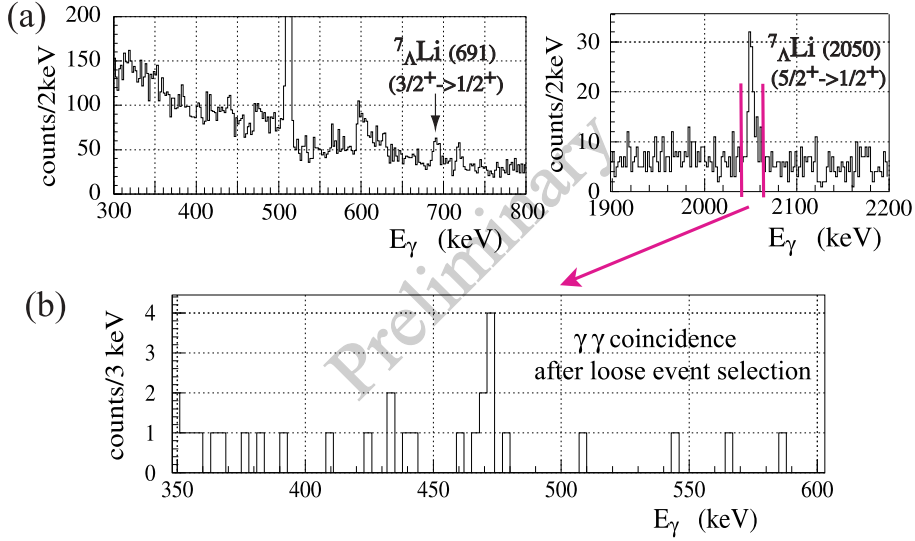


Fig. 5. (a) Preliminary γ -ray spectrum for the unbound region ($0 < -B_\Lambda < 40$ MeV) of $^{10}_\Lambda\text{B}$. Two γ -ray peaks from $^7_\Lambda\text{Li}$ produced as hyperfragments are observed. (b) Preliminary γ -ray spectrum in coincidence with the $^7_\Lambda\text{Li}$ $E2(5/2^+ \rightarrow 1/2^+)$ γ -ray peak. It exhibits a significant peak at 471 keV.

a Λ particle, which was first predicted by Motoba et al.,²⁷⁾ has been experimentally confirmed. It is a good example of “impurity effect” of a Λ particle to nuclear structure, which has become experimentally accessible due to the excellent resolution of γ spectroscopy.

More information on $^7_\Lambda\text{Li}$ was obtained from $^{10}\text{B}(K^-, \pi^-\gamma)$ data taken in an experiment performed later at BNL (E930('01), see §2.5). We observed γ rays from $^7_\Lambda\text{Li}$ produced as hyperfragments from highly excited states of $^{10}_\Lambda\text{B}$, presumably though the s -substitutional $^{10}_\Lambda\text{B}$ (3^+ , ~ 28 MeV excited) state decaying into $^7_\Lambda\text{Li} + ^3\text{He}$ as shown in Fig. 3 (e).^{7), 28)} In the γ -ray spectrum with the unbound region $0 < -B_\Lambda < 40$ MeV of $^{10}_\Lambda\text{B}$ selected (B_Λ denotes the binding energy of a Λ), we observed the $M1(3/2^+ \rightarrow 1/2^+)$ and $E2(5/2^+ \rightarrow 1/2^+)$ γ rays of $^7_\Lambda\text{Li}$ which were previously observed in E419, as shown in Fig. 5 (a). Figure 5 (b) is the spectrum of γ rays emitted in coincidence with the $E2$ γ ray. A peak was clearly observed at 471 keV, which is assigned as the $M1(7/2^+ \rightarrow 5/2^+)$ transition (see Fig. 3 (a)). This is the first successful application of the γ - γ coincidence method to hypernuclei.

This result enables a cross check of the spin-dependent interaction strengths. The doublet ($7/2^+$, $5/2^+$) spacing is mainly determined from both of the spin-spin force (Δ) and the Λ -spin-dependent force (S_Λ), because the core $^6\text{Li}(3^+)$ has the $S = 1, L = 2$ configuration. The observed spacing is consistently explained⁷⁾ with the Δ value determined from the $^7_\Lambda\text{Li}$ ground-state doublet spacing and the very small S_Λ value determined from the $^9_\Lambda\text{Be}$ ($3/2^+, 5/2^+$) doublet spacing described below.

In addition, the change of the core level spacing ($3^+ - 1^+$) in $^7_\Lambda\text{Li}$ is a good measure of the nucleon-spin-dependent spin-orbit force strength (S_N). By taking

the center of gravity for each doublet, the level spacing between the two doublets was obtained to be 1858 keV. It is compared with Millener's shell-model result of

$$\begin{aligned} \overline{E(7/2^+, 5/2^+)} - \overline{E(3/2^+, 1/2^+)} &= E(^6\text{Li}; 3^+) - E(^6\text{Li}; 1^+) \\ &\quad - 0.06\Delta + 0.08S_A + 0.68S_N + 0.05T, \end{aligned}$$

and S_N was derived to be -0.44 MeV almost independently of the other parameters.²⁸⁾

Another interesting result on $^7_\Lambda\text{Li}$ is the determination of the ground-state spin from the yield of the 429 keV ^7Be γ rays emitted after the weak decay of $^7_\Lambda\text{Li} \rightarrow ^7\text{Be}^* + \pi^-$.³⁾ When the bound-state region of $^7_\Lambda\text{Li}$ is selected, the 429 keV γ -ray peak of ^7Be appears prominently as shown in Fig. 4. From the yield of this γ ray, the branching ratio of the $^7_\Lambda\text{Li}$ weak decay to $^7\text{Be}^*(1/2^-, 429 \text{ keV})$ was obtained to be $(6.0^{+1.3}_{-1.6}) \times 10^{-2}$. Because of the much larger non-spin-flip amplitude than the spin-flip amplitude in the $\Lambda \rightarrow N\pi$ decay, the decay into $^7\text{Be}^*(1/2^-)$ dominantly occurs from the $1/2^+$ state of $^7_\Lambda\text{Li}$. The measured large branching ratio indicates that the weakly-decaying ground-state of $^7_\Lambda\text{Li}$ has a spin of $1/2$ but not $3/2$. In fact, the measured branching ratio agrees with the calculated one for spin $1/2$ but is by one order of magnitude larger than the calculated value for spin $3/2$.³⁾

The important observables in $^7_\Lambda\text{Li}$ that remain unmeasured are $B(M1)$ values of the Λ -spin-flip $M1$ transitions of $3/2^+ \rightarrow 1/2^+$ and $7/2^+ \rightarrow 5/2^+$. They provide information of a magnetic moment of a Λ inside a nucleus. They will be measured in future experiments at J-PARC.

2.3. $^9_\Lambda\text{Be}$ and ΛN spin-orbit force

Investigation of the ΛN spin-orbit interaction is particularly important, because it is expected to provide a clue to understand the origin of the nuclear spin-orbit force which is not understood well. Some previous hypernuclear data suggest a very small spin-orbit splitting of Λ single particle states, while some other data suggest a much larger one.²⁹⁾ Thus, high-resolution data for specific hypernuclei such as $^9_\Lambda\text{Be}$ and ^{13}C have been awaited. In the case of $^9_\Lambda\text{Be}$, the energy spacing of the $(5/2^+, 3/2^+)$ doublet based on the $^8\text{Be}(2^+)$ state with $L = 2$ configuration is governed by the Λ -spin-dependent ΛN spin-orbit interaction (S_A).

A γ -ray spectroscopy experiment for $^9_\Lambda\text{Be}$ (BNL E930('98)) was carried out using high-intensity and high-purity kaon beam at the AGS D6 beam line.⁵⁾ $^9_\Lambda\text{Be}$ hypernuclei were produced with the (K^-, π^-) reaction on ^9Be target at $p_{K^-} = 0.93 \text{ GeV}/c$, and γ rays emitted from the hypernuclei were measured with Hyperball.

Figure 6 shows the γ -ray spectrum for the bound-state region in the $^9\text{Be}(K^-, \pi^-)$ $^9_\Lambda\text{Be}$ spectrum. Here, the event-by-event Doppler-shift correction was applied to the previously published spectrum (Fig. 3 in Ref. 5)). The observed structure was well fitted with two peaks of the simulated peak shape for Doppler-shift correction. The peak energies were obtained to be $3024 \pm 3 \pm 1$ and $3067 \pm 3 \pm 1$ keV. The peaks are assigned as the $E2(5/2^+, 3/2^+ \rightarrow 1/2^+)$ transitions in $^9_\Lambda\text{Be}$ (see Fig. 3 (b)). The $(3/2^+, 5/2^+)$ doublet has a spacing of only 43 ± 5 keV, being a typical hypernuclear fine structure.

In the $^9\text{Be}(K^-, \pi^-)$ $^9_\Lambda\text{Be}$ experiment, we cannot assign the spins of $^9_\Lambda\text{Be}$ because

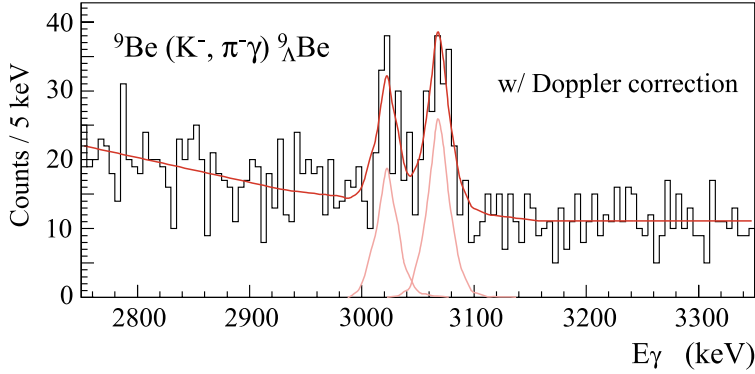


Fig. 6. Measured γ -ray spectrum of ${}^9_{\Lambda}\text{Be}$ after Doppler-shift correction. The twin-peak structure was well fitted using a simulated peak shape for Doppler-shift correction. The two peaks are assigned as the $E2(\frac{5}{2}^+, \frac{3}{2}^+ \rightarrow \frac{1}{2}^+)$ transitions.

of almost equal production cross sections for the $5/2^+$ and $3/2^+$ states. Later, the spin assignment was successful with the ${}^{10}\text{B}(K^-, \pi^-\gamma)$ data taken in E930('01).⁷⁾ In this experiment, the same ${}^9_{\Lambda}\text{Be}$ γ rays were observed when the region of the excitation energy slightly higher than the ${}^{10}\text{B}$ bound-state region was selected. The observed intensity of the upper energy peak (3067 keV) is larger than the lower peak. Considering the production cross sections for ${}^{10}\text{B}$ excited states and their ${}^{10}\text{B} \rightarrow {}^9_{\Lambda}\text{Be} + p$ decay branching ratios, the production rate of the ${}^9_{\Lambda}\text{Be}(3/2^+)$ state is expected to be much larger than that of the ${}^9_{\Lambda}\text{Be}(5/2^+)$ state. Therefore, the $3/2^+$ state is found to be the upper member of the doublet.

This result determines the sign of the spin-orbit force parameter S_{Λ} to be negative. The sign is consistent with the one given by the ${}^{13}\text{C}$ data as described in §2.4. According to a shell-model calculation,²⁵⁾ the spacing is given by

$$E(3/2^+) - E(5/2^+) = -0.037\Delta - 2.464S_{\Lambda} + 0.003S_N + 0.994T + \Lambda\Sigma(\text{MeV}),$$

where $\Lambda\Sigma$ denotes the $\Lambda\Sigma$ coupling effect. Since the term T is obtained to be 0.03 MeV from the ${}^{16}\text{O}$ data described in §2.5, the observed ${}^9_{\Lambda}\text{Be}$ spacing gives a very small spin-orbit strength, $S_{\Lambda} = -0.01$ MeV.

It is much smaller than the value expected from meson-exchange baryon-baryon interaction models through a G-matrix calculation. Recent cluster-model calculations by Hiyama et al.³⁰⁾ using several versions of the meson-exchange baryon-baryon interaction models predicted a spacing of 80 – 200 keV, being much larger than the observation. On the other hand, the ΛN spin-orbit interaction from a quark model gives a small value of 30 keV, which is close to the experimental data.

2.4. ${}^{13}_{\Lambda}\text{C}$ and Λ spin-orbit splitting

The spin-orbit splitting of Λ single particle states in hypernuclei is a direct measure of the Λ -spin-dependent spin-orbit force. Another BNL experiment (E929) was performed in order to measure the spin-orbit splitting of $(p_{1/2})_{\Lambda}$ and $(p_{3/2})_{\Lambda}$ in ${}^{13}_{\Lambda}\text{C}$ by detecting the $E1$ transitions, $(p_{1/2})_{\Lambda} \rightarrow (s_{1/2})_{\Lambda}$ and $(p_{3/2})_{\Lambda} \rightarrow (s_{1/2})_{\Lambda}$ around 11 MeV (see Fig. 3 (c)).⁴⁾ The experiment was carried out with a large-volume NaI

array, which has a much larger efficiency for 11 MeV γ rays than Hyperball. Except for γ -ray detectors the experiment is almost identical to the ${}^9\text{Be}$ experiment with Hyperball. Bound states of ${}^{13}_\Lambda\text{C}$ were populated by 0.93 GeV/c ${}^{13}\text{C}(K^-, \pi^-)$ reaction.

The ${}^{13}_\Lambda\text{C}(1/2^-)$ [${}^{12}\text{C}(0^+) \otimes (p_{1/2})_\Lambda$] state, which is a substitutional ($\Delta L = 0$) state in the (K^-, π^-) reaction, is populated at very forward angles, while the ${}^{13}_\Lambda\text{C}(3/2^-)$ [${}^{12}\text{C}(0^+) \otimes (p_{3/2})_\Lambda$] state requires $\Delta L = 2$ and is populated at backward ($\theta \sim 10^\circ$) angles. Using a magnetic spectrometer having a large angular acceptance ($0^\circ - 12^\circ$), both of the $1/2^-$ and $3/2^-$ states were simultaneously produced without changing the spectrometer setting.

A γ -ray peak was observed at 11 MeV. It was found that the peak energy slightly shifts as a function of the scattering angle, and the $1/2^- - 3/2^-$ splitting was obtained to be $152 \pm 54 \pm 36$ keV as shown in Fig. 3 (c). It is 20–30 times smaller than the $p_{1/2} - p_{3/2}$ spin-orbit splitting of ~ 5 MeV for nucleons. According to Hiyama's calculation³⁰⁾ the meson-exchange interactions give 0.39–0.96 MeV, which is again several times larger than the observed splitting energy as in the ${}^9_\Lambda\text{Be}$ case, and the quark model reproduces the observed splitting.

2.5. ${}^{16}_\Lambda\text{O}$ and ΛN tensor force

The tensor force strength T has been left unknown. Since one-pion exchange, which results in a large tensor force between nucleons, is forbidden between a Λ and a nucleon, the ΛN tensor force is expected to be small. However, kaon exchange and two-pion exchange through the $\Sigma\Lambda$ coupling are expected to give some contribution. The ΛN tensor force can be investigated from the energy spacing of the ground-state doublets in $p_{1/2}$ -shell hypernuclei which have a large contribution of T .

In 2001, ${}^{16}_\Lambda\text{O}$ and ${}^{15}_\Lambda\text{N}$ were studied with Hyperball using the ${}^{16}\text{O}(K^-, \pi^-)$ reaction (BNL E930('01)). See Ref. 6) for details. The setup is almost identical to the previous ${}^9_\Lambda\text{Be}$ experiment. Figure 7 shows the γ -ray spectrum of ${}^{16}_\Lambda\text{O}$. When the bound-state region of ${}^{16}_\Lambda\text{O}$ is selected, the γ -ray spectrum exhibits a broad bump at 6.55 MeV as shown in Fig. 7 (a), while it is not seen in the spectrum for the highly unbound region (Fig. 7 (c)). The bump becomes sharp peaks after event-by-event Doppler-shift correction as shown in Fig. 7 (b). In this reaction, only the 6 MeV-excited 1^- state and the 1^- state in the ground-state doublet are expected to be populated in the ${}^{16}_\Lambda\text{O}$ bound states. Therefore, the observed 6.55 MeV peaks are attributed to the $M1(1^- \rightarrow 1^-, 0^-)$ transitions of ${}^{16}_\Lambda\text{O}$. The widths of the peaks before and after the Doppler-shift correction are consistent with the expected widths for full Doppler broadening due to the expected short lifetime for a 6 MeV $M1$ transition ($\sim 10^{-14}$ s). The peaks in the Doppler-corrected spectrum are fitted with the simulated peak shape, of which width is determined by inaccuracy of Doppler-shift correction. Thus the spacing of the ground-state doublet was obtained to be 26.1 ± 2.0 keV (preliminary). Since the branching ratio of the $1^- \rightarrow 1^-$ to the $1^- \rightarrow 0^-$ decay is 1:2 in the weak coupling limit between a Λ and the core, the γ -ray yield ratio between the two peaks gives spin assignment of the doublet members as shown in Fig. 7. By comparing the present result with a shell-model calculation by Millener, and using already determined values of the spin-dependent parameters (Δ ,

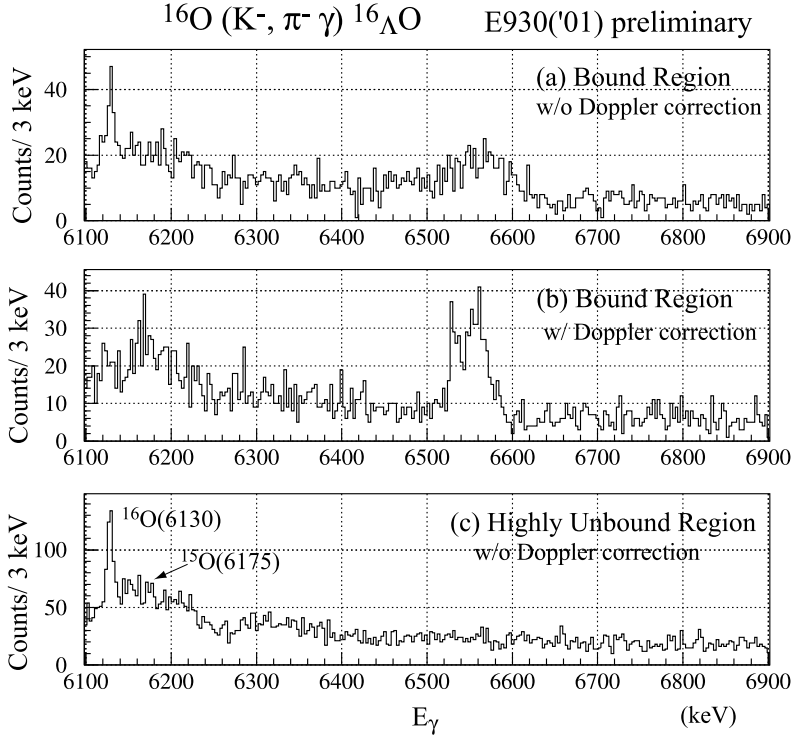


Fig. 7. γ -ray spectrum of $^{16}_{\Lambda}\text{O}$ (preliminary). (a) Bound-state region is gated. (b) Same as (a) but Doppler-shift correction is applied. Twin-peak structure is observed around 6.55 MeV. (c) Highly unbound region is gated.

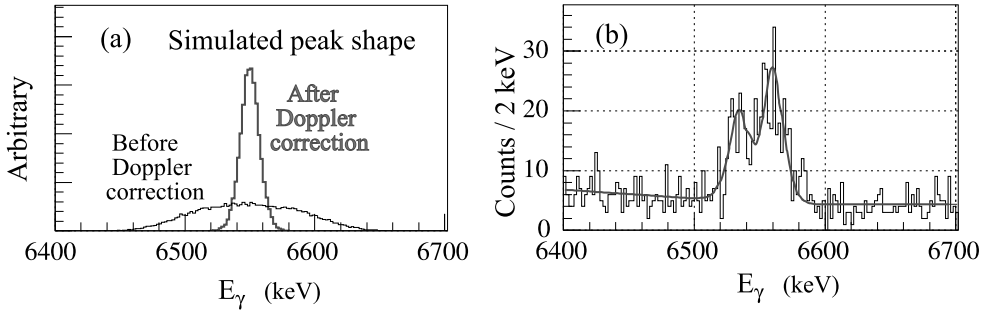


Fig. 8. (a) Simulated peak shape for a fast γ transition before and after Doppler-shift correction. (b) The structure around 6.55 MeV in the $^{16}_{\Lambda}\text{O}$ γ -ray spectrum (Fig. 7 (b)) was fitted with two peaks of the simulated peak shape after Doppler-shift correction.

S_Λ , and S_N), the value of T is derived to be about 30 keV. It is found that the very small doublet spacing is caused by cancellation of the contributions from the spin-spin force and the tensor force.

In addition, by selecting a slightly unbound region of the $^{16}_{\Lambda}\text{O}$ mass, three γ rays were observed.²⁸⁾ They are assigned as the transitions in $^{15}_{\Lambda}\text{N}$ produced by proton emission from the substitutional states of $^{16}_{\Lambda}\text{O}(0^+)$ as shown in Fig. 3 (d).

2.6. ΛN spin-dependent interactions and problems in ${}^{10}_\Lambda B$ and ${}^{11}_\Lambda B$

Through the experiments described above, all the ΛN spin-dependent interaction parameters have been determined as

$$\Delta = 0.43 \text{ MeV}, S_A = -0.01 \text{ MeV}, S_N = -0.44 \text{ MeV}, T = 0.03 \text{ MeV}. \quad (2.2)$$

Let us compare these values with theoretical predictions by various versions (ND, NF, NSC89, NSC97f, etc.) of the Nijmegen meson-exchange interaction through G-matrix calculation.³¹⁾

As for the spin-spin strength Δ , NSC97f (or NSC97e) is favored, which is consistent with the conclusion from s -shell hypernuclei.³²⁾

As described in §§2.3 and 2.4, it is implied that the ΛN spin-orbit force is better explained by quark models rather than meson-exchange models. In terms of S_A and S_N , the Nijmegen interactions give $S_A = -0.13$ — -0.18 MeV and $S_N = -0.26$ — -0.29 MeV, being inconsistent with the experimental values in Eq. (2.2).

On the other hand, meson-exchange picture seems to work well for the ΛN tensor force, because the Nijmegen interactions predict $T = 0.018$ – 0.054 MeV, which almost agree with the experimental value. Moreover, considering ambiguities in the other parameters, the experimental value of T is rather accurately determined as 0.024 – 0.030 MeV.²⁸⁾ It provides a constraint to the property of the tensor force in the meson-exchange models.

The parameter set shown in Eq. (2.2) can also explain most of the other data of p -shell hypernuclei obtained in the recent Hyperball experiments, such as the ${}^7_\Lambda \text{Li}(7/2^+, 5/2^+)$ spacing (Fig. 3 (a)) and the excitation energy of ${}^{16}_\Lambda \text{O}(1_2^-)$ (Fig. 3 (d)).²⁸⁾ However, some of new γ -ray data cannot be well explained by this parameter set. In the ${}^{10}\text{B}(K^-, \pi^-\gamma)$ spectrum in E930('01), a γ -ray peak of the spin-flip $M1$ transition between the ground-state doublet of ${}^{10}_\Lambda \text{B}(2^- \rightarrow 1^-)$ (see Fig. 3 (e)) was not observed,⁷⁾ in spite of high sensitivity of the experiment for this transition, and the limit of $E(2^-) - E(1^-) < 100$ keV was set. It is consistent with the result of an old BNL experiment.³³⁾ The limit of the spacing leads to $\Delta < 0.3$ MeV, being contradictory to the other hypernuclear data supporting $\Delta \sim 0.4$ MeV. It suggests more studies are necessary, particularly on the $\Sigma\Lambda$ coupling effect, to completely understand the ΛN interaction and hypernuclear structure.

Another case is the ${}^{11}_\Lambda \text{B}$ spectrum taken by the (π^+, K^+) reaction at KEK (E518).⁹⁾ This experiment successfully observed six transitions of ${}^{11}_\Lambda \text{B}$, and one of them is assigned as the $E2(1/2^+ \rightarrow 5/2^+)$ transition (see Fig. 3 (f)). The energy of this transition was measured to be 1482 keV, while Millener's shell-model prediction with the already-determined parameter set gives 1020 keV. This rather large difference may be ascribed to the wavefunction of the core nucleus ${}^{10}\text{B}$ having a complicated structure.

§3. $(e, e'K^+)$ spectroscopy

Although γ -ray spectroscopy has achieved an excellent resolution for bound states, spectroscopy of unbound excited states is also important to understand structure of Λ hypernuclei and the ΛN interaction. Since highly-excited Λ single-particle

states generally have much narrower widths than deep hole states of ordinary nuclei with the same excitation energy,³⁴⁾ spectroscopic studies of unbound excited states are particularly useful in hypernuclei.

Reaction spectroscopy of Λ hypernuclei has been pursued mainly by the (π^+, K^+) reaction, which revealed major shell structure of Λ single-particle states in various nuclei³⁵⁾ and core-excited states.³⁶⁾ Because of a large momentum spread and a large dispersion in secondary beams, however, the energy resolution is limited to 1.5 MeV (FWHM), even with the Superconducting Kaon Spectrometer (SKS) at KEK, the best magnetic spectrometer in hypernuclear spectroscopy with secondary beams. A typical hypernuclear spectrum taken by SKS with the (π^+, K^+) reaction is shown in Fig. 9 (top).³⁷⁾

In order to improve the energy resolution further, use of primary beams is in-

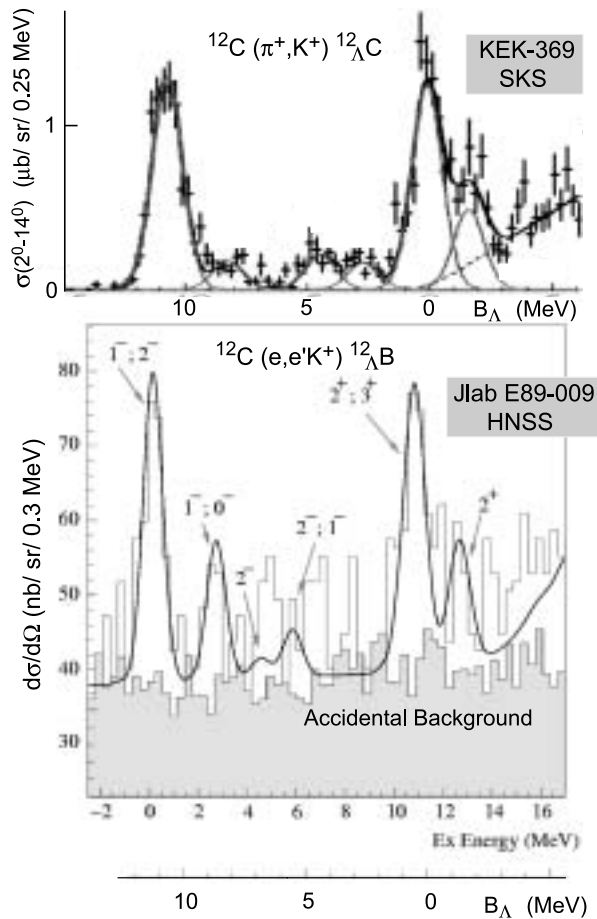


Fig. 9. Excitation spectrum of ${}_{\Lambda}^{12}\text{B}$ measured by the $(e, e'K^+)$ reaction with HNSS at Jefferson Laboratory (bottom),¹⁰⁾ compared with the spectrum of ${}_{\Lambda}^{12}\text{C}$ by the (π^+, K^+) reaction with SKS at KEK-PS (top).³⁷⁾ The energy resolution has been improved from 1.5 MeV (FWHM) to 0.9 MeV (FWHM) by the $(e, e'K^+)$ reaction. In the bottom spectrum, the solid curve shows a theoretically calculated spectrum (see Ref. 10)).

dispensable. The high-intensity electron beam at Thomas Jefferson National Accelerator Facility has enabled high-resolution hypernuclear spectroscopy with primary beams. The first experiment using the $(e, e'K^+)$ reaction (E89-009) was recently performed. Irradiating 1.8 GeV electron beam and analyzing a scattered electron and K^+ both emitted at around zero degree, the ${}_{\Lambda}^{12}\text{B}$ spectrum was successfully obtained and the two peaks corresponding to the s_{Λ} and p_{Λ} states were observed with a resolution of 0.9 MeV (FWHM) as shown in Fig. 9 (bottom).¹⁰⁾ This is the best energy resolution achieved so far in reaction spectroscopy of hypernuclei. The cross sections of the ${}_{\Lambda}^{12}\text{B}$ states are well reproduced by a DWIA calculation as shown in a solid curve in Fig. 9 (see Ref. 10) for details).

Since this reaction induced by virtual photons has a large spin-flip amplitude in converting a proton to a Λ , spin-flip states of hypernuclei can be populated. It is in contrast to the conventional (π^+, K^+) and (K^-, π^-) reactions having a large non-spin-flip amplitude. In addition, this reaction produces mirror hypernuclei of those produced by the (π^+, K^+) and (K^-, π^-) reactions which convert a neutron into a Λ . It can also produce neutron-rich hypernuclei such as ${}_{\Lambda}^7\text{He}$, ${}_{\Lambda}^9\text{Li}$ and ${}_{\Lambda}^{11}\text{Be}$.

A dedicated magnetic spectrometer called High-resolution Kaon Spectrometer (HKS) has recently been constructed.³⁸⁾ With this spectrometer, systematic studies of various hypernuclei from very light ones to medium-heavy ones will start soon at Jefferson Laboratory. This spectrometer will allow us to take hypernuclear spectra with an excellent resolution of 0.4 MeV (FWHM), with much less background, and of statistics more than 50 times larger than with the previous spectrometer (HNSS).

§4. Neutron-rich hypernuclei with the (π^-, K^+) reaction

One of the recent new challenges in hypernuclear spectroscopy is the study of neutron-rich hypernuclei with the (π^-, K^+) reaction. In this reaction, two protons are converted to a Λ and a neutron via the two-step charge exchange reaction ($\pi^-p \rightarrow K^0\Lambda$, $K^0p \rightarrow K^+n$ or $\pi^-p \rightarrow \pi^0n$, $\pi^0p \rightarrow K^+\Lambda$) or the $\Sigma\Lambda$ mixing ($\pi^-p \rightarrow K^+\Sigma^-$, $\Sigma^-p \leftrightarrow \Lambda n$). Recently, Akaishi predicted a ‘‘hyperheavy hydrogen’’ ${}_{\Lambda}^6\text{H}$, of which ground state is expected to be deeply bound due to the coherent $\Sigma\Lambda$ coupling.³²⁾ In such neutron-rich hypernuclei, the coherent $\Sigma\Lambda$ coupling is expected to play an important role in the level energies and the production cross section.

The experiment (E521) was carried out to produce a neutron-rich hypernucleus ${}_{\Lambda}^{10}\text{Li}$ with the ${}^{10}\text{B}(\pi^-, K^+){}_{\Lambda}^{10}\text{Li}$ reaction using the KEK-PS K6 beam line and SKS with 1.05 and 1.2 GeV/ c pion beams. See Ref. 11) for details. A preliminary spectrum shown in Fig. 10 exhibited a significant number of events in the bound region for ${}_{\Lambda}^{10}\text{Li}$. This is the first evidence of neutron-rich hypernuclei produced by the (π^-, K^+) reaction. The total cross section for the bound states is about 1×10^{-3} of the cross section of the ${}^{12}\text{C}(\pi^+, K^+){}_{\Lambda}^{12}\text{C}$ (ground state) at 1.05 GeV/ c ($8 \mu\text{b}/\text{sr}$ for 2° – 14°). It is about an order of magnitude lower than a theoretical value for the two-step charge-exchange reaction. The cross section was found to be much larger with 1.2 GeV/ c beam than 1.05 GeV/ c . It implies a possible large contribution of the $\Sigma\Lambda$ mixing, because the two-step charge-exchange reaction is expected to have a largest cross section at 1.05 GeV/ c while the Σ production has a larger cross section

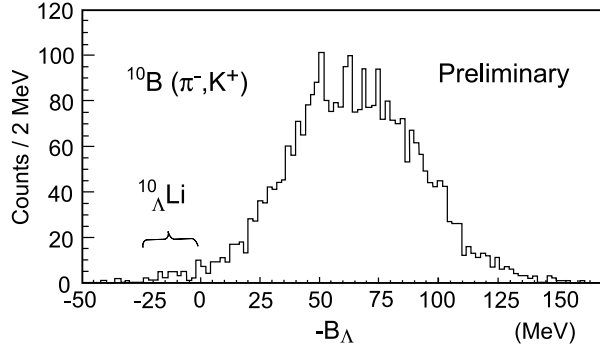


Fig. 10. Preliminary spectrum of $^{10}\text{B}(\pi^-, K^+)^{10}_{\Lambda}\text{Li}$ reaction with 1.2 GeV/c π^- beam measured at KEK (E521). Events for the bound states of $^{10}_{\Lambda}\text{Li}$ are observed.

at 1.2 GeV/c.

Such studies of neutron-rich hypernuclei via the (π^-, K^+) reaction are planned in the high-resolution and high-intensity pion beam line at J-PARC.

§5. Double Λ hypernuclei

Experimental information on double strangeness nuclear system has been quite scarce. Double Λ hypernuclei were claimed to be observed in old emulsion experiments in 1960's.^{39),40)} Later in 1990's, a reliable result for observation of a double hypernuclear event was reported with an emulsion-counter hybrid experiment at KEK (E176).⁴¹⁾

The existence of weakly-decaying double Λ hypernuclei is an evidence against the existence of a bound H dibaryon lighter than two Λ 's. Furthermore, the binding energy of a double Λ hypernucleus provides the $\Lambda\Lambda$ interaction energy as $\Delta B_{\Lambda\Lambda} = B_{\Lambda\Lambda}(^A_{\Lambda\Lambda}Z) - 2B_{\Lambda}(^A_{\Lambda}Z)$, where $B_{\Lambda\Lambda}$ is the binding energy of two Λ 's in a double hypernucleus. $\Delta B_{\Lambda\Lambda}$ gives information related to a possible strongly attractive interaction in the H dibaryon channel (the $SU(3)_f \times SU(3)_f$ singlet state) of two strange baryons.

In the previous hybrid emulsion experiment (E176), 80 events of Ξ^- absorption at rest were identified in emulsion by tracing Ξ^- tracks from (K^-, K^+) vertices which were predicted with information from counters and magnetic spectrometers. Among those events, one light double Λ hypernuclear event showing sequential weak decays were found,⁴¹⁾ although the double hypernuclear species cannot be uniquely identified. Unambiguous determination of $\Delta B_{\Lambda\Lambda}$ from a uniquely-identified double hypernucleus without ambiguity of γ -emitting excited states has been awaited.

5.1. Double Λ hypernuclei identified by sequential pion decays

Recently, two experiments reported observation of double Λ hypernuclei. One is a counter-type experiment carried out at BNL (E906). Using a cylindrical spectrometer (CDS) around the target, two π^- 's from sequential weak decay of light double hypernuclei were detected in coincidence with the (K^-, K^+) reaction on ^9Be target.

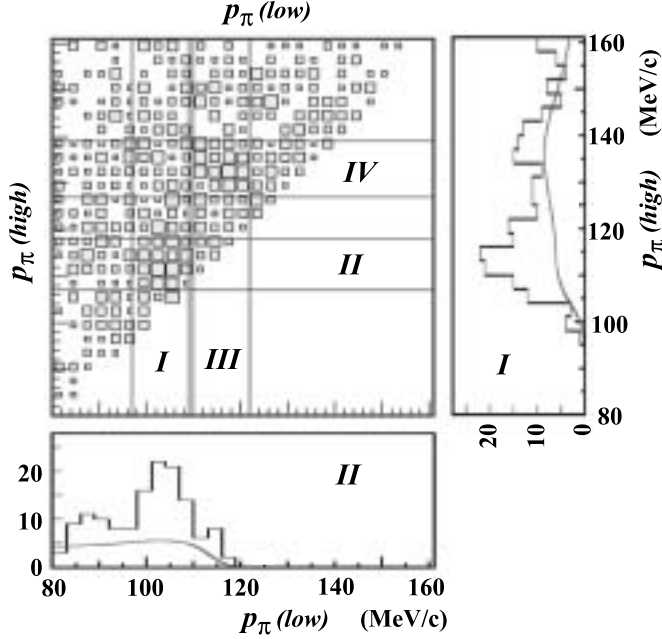


Fig. 11. Correlation of the momenta of two π^- 's emitted from ${}^9\text{Be}(K^-, K^+)$ reaction, $p_{\pi}(\text{high})$ and $p_{\pi}(\text{low})$, measured in BNL E906. Projections in the region I and II are also shown. The correlated peak events for $(p_{\pi}(\text{high}), p_{\pi}(\text{low})) = (114, 104)$ MeV/c are interpreted as the sequential π^- decay of ${}^4_{\Lambda\Lambda}\text{H}$ (see text).¹²⁾

See Ref. 12) for details.

In this experiment, double Λ hypernuclei are produced as hyperfragments by absorption of Ξ^- following the “ p ”(K^-, K^+) Ξ^- reaction, or directly by the (K^-, K^+) reaction. Since the mesonic decay of a single Λ hypernucleus is often a two-body decay (${}^A_{\Lambda}Z \rightarrow {}^A[Z+1] + \pi^-$ or ${}^A[Z+1]^* + \pi^-$), the π^- mostly has a monochromatic or a nearly monochromatic momentum characteristic to the hypernuclear species. Similarly, monochromatic π^- emission is often expected in the decay of a double hypernucleus to a single hypernucleus. Once a single hypernucleus is identified, the momentum of the other monochromatic π^- gives the parent double hypernuclear species and its binding energy.

Figure 11 is the scatterplot for the momenta of two π^- 's ($p(\text{high})$ and $p(\text{low})$). A peak was observed at $(p(\text{high}), p(\text{low})) = (114, 104)$ MeV/c. The momentum of 114 MeV/c agrees with the pion momentum in ${}^3_{\Lambda}\text{H} \rightarrow {}^3\text{He} + \pi^-$ decay. In this case, the only possible parent double hypernucleus is ${}^4_{\Lambda\Lambda}\text{H}$; ${}^4_{\Lambda\Lambda}\text{H}$ is considered to decay to ${}^4_{\Lambda}\text{He}^* + \pi^-$ by emitting a 104 MeV/c pion, and the ${}^4_{\Lambda}\text{He}^*$ resonance breaks up into ${}^3_{\Lambda}\text{H} + p$. This resonance is not observed yet but expected to exist.⁴²⁾ Because of the unknown excitation energy of the ${}^4_{\Lambda}\text{He}^*$ resonance, $\Delta B_{\Lambda\Lambda}$ cannot be derived. However, it is found that the existence of H dibaryon with a mass less than a few MeV below the two Λ mass is unlikely.

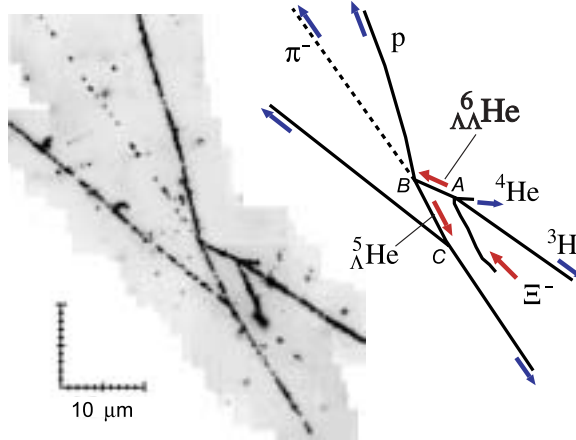


Fig. 12. Emulsion image of Nagara event detected in the hybrid emulsion experiment, KEK E373.¹³⁾ Sequential weak decay of ${}^6_{\Lambda\Lambda}\text{He}$ was observed as illustrated in the right figure (see text).

5.2. Nagara event

The other successful experiment is an improved hybrid emulsion experiment (KEK E373) with scintillating fiber detectors (SCIFI) which are used to trace Ξ^- from the (K^-, K^+) reaction point in the target to the Ξ^- absorption point in the emulsion stack.

In 1×10^3 Ξ^- absorption events recorded in emulsion, three distinct events of double Λ hypernuclei have been observed.¹³⁾ Among them, the event called ‘‘Nagara’’ (Fig. 12) exhibits a uniquely-identified double Λ hypernucleus without ambiguity of excited states.

This event was uniquely interpreted as given in Fig. 12 (right), namely, $\Xi^- {}^{12}\text{C} \rightarrow {}^6_{\Lambda\Lambda}\text{He} {}^4\text{He} {}^3\text{H}$ at point A, ${}^6_{\Lambda\Lambda}\text{He} \rightarrow {}^5_{\Lambda}\text{He} \pi^- p$ at point B, and ${}^4\text{He} \rightarrow p d 2n$ etc. at point C. The double hypernucleus ${}^6_{\Lambda\Lambda}\text{He}$, called *Lampha*, is a triple closed-shell nucleus and does not have γ -emitting excited states. Any other nuclei participating in the production (point A) and the decay (point B) of ${}^6_{\Lambda\Lambda}\text{He}$ have no γ -emitting excited states either. Therefore, the binding energy of ${}^6_{\Lambda\Lambda}\text{He}$ ($B_{\Lambda\Lambda}$) was obtained unambiguously from both production and decay, and the $\Lambda\Lambda$ interaction energy was determined to be $\Delta B_{\Lambda\Lambda} = 1.01 \pm 0.20^{+0.18}_{-0.11}$ MeV. Thus the interaction between two Λ 's was found to be weakly attractive. This is the first reliable result on the $\Lambda\Lambda$ interaction energy. This value of $\Delta B_{\Lambda\Lambda}$ is much smaller than the previously reported value of 4 MeV (strongly attractive) from the old emulsion event.⁴⁰⁾ The determined $\Lambda\Lambda$ interaction strength gives a crucial effect to properties of hyperonic nuclear matter in neutron stars.

It is pointed out that structure change of the core nucleus induced by two Λ 's affects the $\Delta B_{\Lambda\Lambda}$ value dependently on the core nuclear structure.⁴³⁾ Therefore, more experimental data for various double hypernuclei are necessary to confirm the $\Lambda\Lambda$ interaction energy. Moreover, such accumulated data will allow us to investigate the $\Lambda\Lambda - \Xi N$ coupling effect. For this purpose, further experiments with the sequential

pion method and the hybrid emulsion method are planned at BNL and then at J-PARC.

§6. Weak decay of hypernuclei — Solution of the Γ_n/Γ_p ratio puzzle

The nonmesonic weak decay of Λ hypernuclei is an interesting process of purely baryonic weak interaction which reflects the YN strong interactions including short-range forces. Theoretical studies based on meson exchanges and quark-quark interactions have been made, but experimental observables cannot be explained well.⁴⁴⁾ In particular, there has been a long-standing puzzle that the ratio between the neutron-stimulated decay rate $\Gamma_n = \Gamma(\Lambda n \rightarrow nn)$ and the proton-stimulated decay rate $\Gamma_p = \Gamma(\Lambda p \rightarrow np)$, called the Γ_n/Γ_p ratio, and the total nonmesonic decay rate $\Gamma_{NM} = \Gamma_n + \Gamma_p$ cannot be simultaneously reproduced by any of theoretical models. Because of a large contribution of pion exchange which makes a tensor force responsible only to the $\Lambda p \rightarrow np$ process, theoretical predictions of the Γ_n/Γ_p ratio are of the order of 0.1, while previous experiments reported values around unity.⁴⁴⁾

In the previous experiments, however, there were problems. One of them is inaccuracy in estimating Γ_n without measuring neutrons, or a large error in Γ_n caused by a difficulty in measuring neutrons. Another one is the effect of rescattering of protons and neutrons inside the same nucleus which changes their energy distributions and yields.

In order to solve these problems, measurement of neutrons with high efficiency detectors is necessary, and it is desirable to make an exclusive measurement to select events in which almost no rescattering of nucleons takes place inside the nucleus. For this purpose, the KEK experiments E462 and E508 were recently carried out. Employing the K6 beam line and SKS, ${}^5_\Lambda\text{He}$ and ${}^{12}_\Lambda\text{C}$ hypernuclei were produced and identified by the (π^+, K^+) reaction on ${}^6\text{Li}$ and ${}^{12}\text{C}$ targets, respectively, and neutrons as well as protons and pions emitted from hypernuclear weak decay were detected with three large stacks of plastic counters installed at 90° and 180° to each other from the target.

The energy spectra of neutrons and protons were measured with high statistics. Even for ${}^5_\Lambda\text{He}$, their energies do not distribute around the half of the Q-value (~ 75 MeV) of the $\Lambda N \rightarrow NN$ process, and a large number of nucleons with lower energies were observed. It may suggest a large effect of rescattering. When high energy (> 60 MeV) components of protons and neutrons were selected to suppress rescattering events, the proton and neutron energy spectra look similar and the yield ratio of neutrons to protons was found to be almost 2 for both of ${}^5_\Lambda\text{He}$ and ${}^{12}_\Lambda\text{C}$. It corresponds to the Γ_n/Γ_p ratio of ~ 0.5 (preliminary).^{15),16)}

In the $n-p$ and $n-n$ coincidence measurement, the measured angular correlation has a peak at 180° corresponding to back-to-back decay, when both nucleon energies are required to be larger than 30 MeV, as shown in Figs. 13 (a) and (c). Then the 180° peak events ($\cos\theta_{NN} < -0.8$) were selected to exclude rescattering events. For these selected events, the energy sum of the two nucleons distributes around the Q-value of 150 MeV as shown in Figs. 13 (b) and (d), demonstrating that non-rescattering events are properly selected. For these events, the ratio of the $n-n$

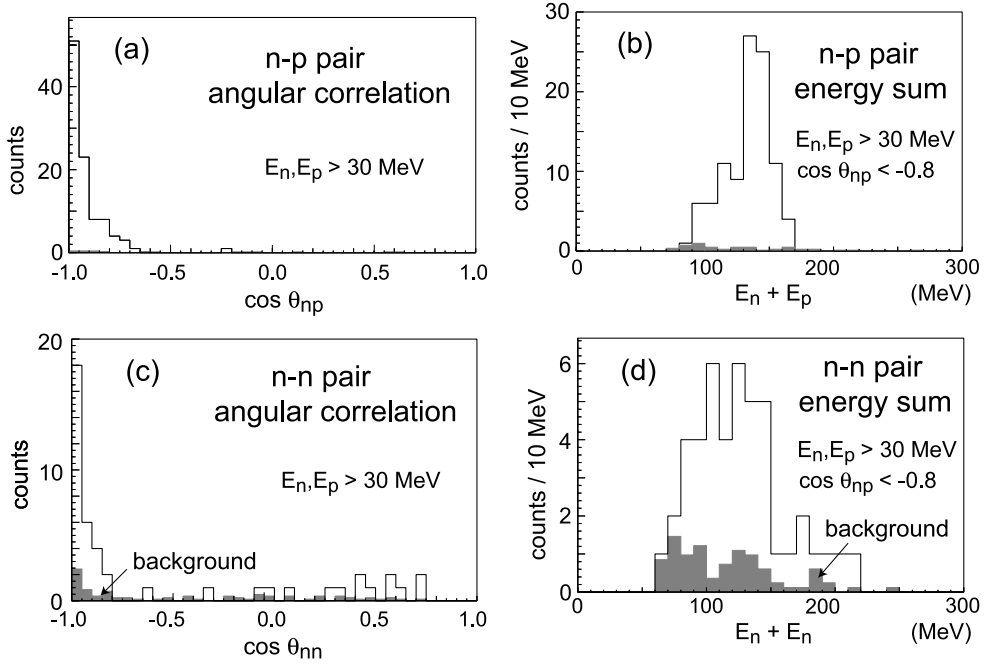


Fig. 13. Results of $n - p$ and $n - n$ coincidence measurements for ${}^5_{\Lambda}\text{He}$ nonmesonic weak decay (preliminary). (a) Angular correlation between n and p with both energies larger than 30 MeV. (b) Energy sum of n and p for back-to-back ($\cos \theta_{np} < -0.8$) events selected in (a). (c) and (d) are the same as (a) and (b), respectively, but for $n - n$ pair.

yield to the $n - p$ yield was obtained to be $0.45 \pm 0.11 \pm 0.04$ (preliminary) for ${}^5_{\Lambda}\text{He}$. It gives the most reliable value for the Γ_n/Γ_p ratio.^{15),17)}

This result is significantly smaller than the previously reported values. A recent theoretical calculation based on meson-exchange mechanism together with internuclear cascade process predicts a value of $\Gamma_n/\Gamma_p \sim 0.5$ as the ratio of $n - n/n - p$ coincidence counts.⁴⁵⁾ Therefore, the long-standing puzzle of the Γ_n/Γ_p ratio has been solved.

These KEK experiments measured the lifetimes of ${}^5_{\Lambda}\text{He}$ and ${}^{12}_{\Lambda}\text{C}$, as well as the yields and the energy spectra of neutrons, protons, π^- and π^0 from their weak decays, so that the decay rate of each decay mode and the asymmetry parameter in nonmesonic decay can be measured precisely for both ${}^5_{\Lambda}\text{He}$ and ${}^{12}_{\Lambda}\text{C}$.¹⁵⁾

§7. Future

At Jlab, a full-scale investigation of high-resolution ($e, e'K^+$) spectroscopy will start in 2005 with a high-resolution and large-acceptance spectrometer, HKS.

The FINUDA experiment in DAFNE has started data-taking and will provide not only Λ hypernuclear spectra with a good resolution (< 1 MeV) but also high quality data on their weak decays.

The most important facility in strangeness nuclear physics in the coming decade

is the high-intensity proton synchrotron facility, J-PARC. Using intense and pure K^- beams of 1–2 GeV/c region, we plan to carry out various programs on strangeness nuclear physics, such as high-precision γ -ray spectroscopy of Λ hypernuclei, Ξ hypernuclear spectroscopy with the (K^-, K^+) reaction, studies of double Λ hypernuclei with the sequential π^- decay method and the improved hybrid emulsion method, investigation of kaonic nuclear bound states, and so on.

§8. Summary

In these five years, various experimental progress has been made in hypernuclear physics. γ -ray spectroscopy of Λ hypernuclei with a germanium detector array (Hyperball) as well as an NaI counter array has revealed level structure of various p -shell Λ hypernuclei and allowed us to extract information on all the spin-dependent ΛN interactions. Spectroscopy of Λ hypernuclei by the $(e, e'K^+)$ reaction was first successful at Jlab with an energy resolution less than 1 MeV (FWHM). At KEK, an experiment to produce neutron-rich hypernuclei by the (π^-, K^+) reaction has been carried out. As for double strangeness systems, a double Λ hypernucleus interpreted as ${}^4_{\Lambda\Lambda}\text{H}$ was observed at BNL from correlated two monochromatic π^- 's. In the emulsion-counter hybrid experiment at KEK, a double Λ hypernucleus ${}^6_{\Lambda\Lambda}\text{He}$ was observed and the $\Lambda\Lambda$ interaction strength was unambiguously derived for the first time. In the study of weak decay, the so-called Γ_n/Γ_p ratio puzzle has been solved by measuring $n - p$ and $n - n$ angular correlation with large-volume neutron counters.

References

- 1) H. Tamura et al., Phys. Rev. Lett. **84** (2000), 5963.
- 2) K. Tanida et al., Phys. Rev. Lett. **86** (2001), 1982.
- 3) J. Sasao et al., Phys. Lett. B **579** (2004), 258.
- 4) S. Ajimura et al., Phys. Rev. Lett. **86** (2001), 4255.
- 5) H. Akikawa et al., Phys. Rev. Lett. **88** (2002), 082501.
- 6) M. Ukai et al., *Proc. Int. Conf. on Hypernuclear and Strange Particle Physics (HYP2003)*, Jefferson Lab., October 14-18, 2003, Nucl. Phys., in press.
- 7) H. Tamura et al., *Proc. Int. Conf. on Hypernuclear and Strange Particle Physics (HYP2003)*, Jefferson Lab., October 14-18, 2003, Nucl. Phys., in press.
- 8) K. Tanida et al., Nucl. Phys. A **721** (2003), 999c.
- 9) Y. Miura et al., *Proc. Int. Conf. on Hypernuclear and Strange Particle Physics (HYP2003)*, Jefferson Lab., October 14-18, 2003, Nucl. Phys., in press.
- 10) T. Miyoshi et al., Phys. Rev. Lett. **90** (2003), 232502.
- 11) P. K. Saha et al., *Proc. Int. Conf. on Hypernuclear and Strange Particle Physics (HYP2003)*, Jefferson Lab., October 14-18, 2003, Nucl. Phys., in press.
- 12) J. K. Ahn et al., Phys. Rev. Lett. **87** (2001), 132504.
- 13) H. Takahashi et al., Phys. Rev. Lett. **87** (2001), 212502.
- 14) R. L. Gill et al., Nucl. Phys. A **691** (2001), 180c.
- 15) B. C. Bhang, *Proc. Int. Conf. on Hypernuclear and Strange Particle Physics (HYP2003)*, Jefferson Lab., October 14-18, 2003, Nucl. Phys. to be published.
H. Outa, *Proc. Int. Conf. on Hypernuclear and Strange Particle Physics (HYP2003)*, Jefferson Lab., October 14-18, 2003, Nucl. Phys., to be published.
- 16) S. Okada et al., to be published.
- 17) B. H. Kang et al., to be published.
- 18) H. Noumi et al., Phys. Rev. Lett. **89** (2002), 072301.
- 19) Y. Kondo et al., Nucl. Phys. A **676** (2000), 371.

- 20) T. Kadowaki et al., *Eur. Phys. J. A* **15** (2002), 295.
- 21) T. Kishimoto et al., *Proc. Int. Conf. on Hypernuclear and Strange Particle Physics (HYP2003)*, Jefferson Lab., October 14-18, 2003, *Nucl. Phys.*, to be published.
- 22) T. Suzuki et al., *Proc. Int. Conf. on Hypernuclear and Strange Particle Physics (HYP2003)*, Jefferson Lab., October 14-18, 2003, *Nucl. Phys.*, to be published.
- 23) R. H. Dalitz and A. Gal, *Ann. of Phys.* **116** (1978), 167.
- 24) D. J. Millener, A. Gal, C. B. Dover and R. H. Dalitz, *Phys. Rev. C* **31** (1985), 499.
- 25) D. J. Millener, *Proc. Int. Conf. on Hypernuclear and Strange Particle Physics (HYP2003)*, Jefferson Lab., October 14-18, 2003, *Nucl. Phys.*, in press.
- 26) E. Hiyama, M. Kamimura, K. Miyazaki and T. Motoba, *Phys. Rev. C* **59** (1999), 2351.
- 27) T. Motoba, H. Bandō and K. Ikeda, *Prog. Theor. Phys.* **70** (1983), 189.
- 28) M. Ukai, Ph.D. thesis, Tohoku University, 2004.
- 29) See references in Ref. 4) or Ref. 5).
- 30) E. Hiyama et al., *Phys. Rev. Lett.* **85** (2000), 270.
- 31) D. J. Millener, *Proc. Jlab Sponsored Workshop on Hypernuclear Physics with Electromagnetic Probes*, Hampton, December 2-4, 1999, ed. L. Tang and O. Hashimoto, p. 79.
- 32) Y. Akaishi et al., *Phys. Rev. Lett.* **84** (2000), 3539.
- 33) R. E. Chrien et al., *Phys. Rev. C* **41** (1990), 1062.
- 34) H. Bandō, T. Motoba and Y. Yamamoto, *Phys. Rev. C* **31** (1985), 265.
- 35) P. H. Pile et al., *Phys. Rev. Lett.* **66** (1991), 2585.
T. Hasegawa et al., *Phys. Rev. C* **53** (1996), 1210.
- 36) T. Hasegawa et al., *Phys. Rev. Lett.* **74** (1995), 224.
- 37) H. Hotchi et al., *Phys. Rev. C* **64** (2001), 044302.
- 38) Y. Fujii et al., *Nucl. Phys. A* **721** (2003), 1079c.
- 39) M. Danysz et al., *Nucl. Phys.* **49** (1963), 121.
- 40) D. J. Prowse et al., *Phys. Rev. Lett.* **17** (1966), 782.
- 41) S. Aoki et al., *Prog. Theor. Phys.* **85** (1991), 1287.
- 42) D. E. Kahana, S. H. Kahana and D. J. Millener, *Phys. Rev. C* **68** (2003), 037302.
- 43) E. Hiyama et al., *Phys. Rev. C* **66** (2002), 024007.
- 44) See references in Ref. 15).
- 45) G. Garbarino, A. Parreño and A. Ramos, *Phys. Rev. Lett.* **91** (2003), 112501.